Sensitivity Function Computation of Electrical Resistance Imaging Using Forward Matrix Method

Reza Ghanati[1]

[1]Assitant professor of Institute of geophysics, University of Tehran; rghanati@ut.ac.ir

ABSTRACT

The sensitivity matrix is an integral part of every non-linear inversion process. The sensitivity values indicate the variation of the forward response with respect to the variation of model parameters. Sensitivity patterns are also a criterion to assess the reliability of the inverted models and to design optimum resistivity surveys. In this study, a numerical approach based on the forward matrix calculation in the framework of the 2.5D finite-difference electrical resistivity forward modeling is presented. To verify and analyze the proposed numerical method, the sensitivity distributions assuming homogeneous and inhomogeneous media for commonly used electrical resistivity tomography configurations (e.g. pole-pole, pole-dipole, dipole-dipole, and Wenner) are computed. The numerical experiments reveal that the sensitivity patterns vary spatially throughout the model depending not only on the resistivity distribution but also on the electrode configuration.

Keywords: Electrical resistivity imaging; Sensitivity function; Finite difference method

INTRODUCTION

The inversion of electrical resistivity tomography provides an image of the subsurface conductivity distribution in near-surface investigations. The inverse solution of resistivity data requires knowledge about the Fréchet derivatives (sensitivity values) constructing the elements of the Jacobian matrix of the objective function. These sensitivity values denote the change in electrical potential or apparent conductivity due to a change in subsurface conductivity or resistivity distribution. The greater the value of the sensitivity function, the higher is the influence of the subsurface medium on the potential measured by the electrical array. In other words, through the comparison of the derivative values for the individual data with respect to all model parameters, it is possible to give a concept of how the physical properties can be distinguished from each other. Thus, the sensitivity analysis provides the possibility of optimizing field survey design and computation of resolution matrices. The dimension of the sensitivity matrix depends upon the size of the discretized model (i.e., model space) and the number of the electrode displacements so that each element of the matrix contains only the neighboring conductivities of the corresponding cell and for each model cell all current sources have to be considered leading to solving $m_d \times n_m$ single forward problem. The first attempts of the Fréchet derivatives calculation for resistivity modeling are in conjunction with inversion approaches. McGillivray and Oldenburg (1990) presented a comparison of three approaches for calculating the sensitivity matrix for a 2D and 3D earth. Spitzer (1998) described derivatives for various electrode arrays at the surface and subsurface (cross-hole measurements) on 3D models using analytic and numerical schemes. Loke and Barker (1995) developed a numerical method for the solution of the Fréchet derivative integral on a homogeneous half-space. Günther et al (2006) used the reciprocity theorem to numerically compute the sensitivity function. Szalai and Szarka (2008) dealt with sensitivity patterns in isotropic and homogeneous earth for some non-conventional arrays. Despite successful publications for the solution of the sensitivity function, it is still an interesting research area to investigate in detail. The main motivation behind this study, in addition to providing an accurate and fast calculation approach of the sensitivity function, is to further deal with sensitivity properties of the conventional geo-electrical arrangements from the computational and theoretical aspects. Thus, a numerical strategy based on the forward matrix method in the framework of a finite difference approach is presented.

METHODOLOGY

In general, to determine the DC sensitivity in 2.5D and 3D models, there are three numerical schemes including the adjoint equation approach, perturbation method, forward matrix technique, and one analytic method. The numerical ones are applied to arbitrary resistivity structures while the analytic one is basically used for homogeneous models. In this section, to compute sensitivity with respect to an arbitrary conductivity distribution in an isotropic medium, we focus on providing a formulation of the DC forward matrix method. The governing equation of the DC electrical potential due to a point current source in 3D isotropic and inhomogeneous media is stated in terms of the partial differential equation as

$$\boldsymbol{\nabla}\cdot[\sigma(x.y.z)\boldsymbol{\nabla}\mathrm{U}(x.y.z)] = -I\delta(x-x_s)\delta(y-y_s)\delta(z-z_s) \tag{1}$$

Where I is the current intensity injected into the subsurface, σ stands for the arbitrary distribution of subsurface conductivity, U is the potential distribution due to a point source, and x_s, y_s, and z_s display the position of the surface source.
Taking into account the 2.5D modeling assumptions (i.e., 3D current source and 2D resistivity variation), Equation (1) becomes

$$\boldsymbol{\nabla}\cdot[\sigma(x.z)\boldsymbol{\nabla}\mathrm{U}(x.y.z)] = -I\delta(x-x_s)\delta(y-y_s)\delta(z-z_s) \tag{2}$$

To account for the 3D source characteristic, the three-dimensionality of the point source is transformed into wavenumber domain through a spatial Fourier transform of the partial differential equations along the strike direction. The corresponding transformation of Equation (2) yields

$$\boldsymbol{\nabla}\cdot\left[\sigma(x.z)\boldsymbol{\nabla}\tilde{U}\left(x.k_y.z\right) - k_y^2\sigma(x.z)\boldsymbol{\nabla}\tilde{U}\left(x.k_y.z\right)\right] = -\frac{I}{2}\delta(x-x_s)\delta(z-z_s) \tag{3}$$

Where $\tilde{\mathrm{U}}$ denotes the transformed potential and k_y is the wavenumber with respect to the direction y. Considering a mixed-boundary conditions, the partial deferential equation (Eq. 3) is solved by the method of finite difference. Hence, the numerical solution of the differential equations results in the system of algebraic equations as

$$\boldsymbol{C}\tilde{\boldsymbol{u}}(x,k_y,z) = \boldsymbol{q} \tag{4}$$

Where $\boldsymbol{C}$ is the coupling matrix affected by the subsurface conductivity distribution and discretization properties and $\boldsymbol{q}$ stands for the vector of source. Note that the solution of the above symmetric and positive definite set of linear equations will give the transformed potential $\tilde{\boldsymbol{u}}(x,k_y,z)$ for specified values of k. In order to derive the potential in the spatial domain ($\boldsymbol{u}(x,z)$) the inverse Fourier transform should be applied. Hence, a shape-preserving piecewise cubic interpolation algorithm is applied to approximate the integration between the smallest and largest wavenumbers. We refer to Ghanati et al (2020) for the basics and mathematical background of 2.5-D DC resistivity forward calculations.
To obtain the sensitivity quantities, it is required to differentiate Equation (4) with respect to the $n$the conductivity σ_n which yields (the source term is independent of σ_n, then $\frac{\partial \boldsymbol{q}}{\partial \sigma_n} = 0$)

$$\frac{\partial \boldsymbol{C}}{\partial \sigma_n}\tilde{\boldsymbol{u}}(x,k_y,z) + \boldsymbol{C}\frac{\partial \tilde{\boldsymbol{u}}(x,k_y,z)}{\partial \sigma_n} = 0 \tag{5}$$

For simplicity

$$\boldsymbol{C}'\tilde{\boldsymbol{u}}(x,k_y,z) + \boldsymbol{C}\tilde{\boldsymbol{u}}'(x,k_y,z) = 0 \tag{6}$$

From the above equation, with the assumption that the matrix $\boldsymbol{C}'$ is known and $\boldsymbol{C}$ and $\tilde{\boldsymbol{u}}(x,k_y,z)$ are computed from the forward calculations, the objective is to determine $\tilde{\boldsymbol{u}}'(x,k_y,z)$ on every wavenumber in the Fourier space. After deriving every wavenumber, an inverse Fourier transform is required to convert $\tilde{\boldsymbol{u}}'(x,k_y,z)$ in Fourier space to $\boldsymbol{u}'(x,z)$ in spatial space.

NUMERICAL EXAMPLES

The sensitivity patterns of homogeneous and inhomogeneous models, including a uniform resistivity model and rectangular body buried in a high resistive half-space medium, with respect to different electrical arrays, e.g. pole-pole, pole-dipole, dipole-dipole, and Wenner, are presented.

a) Homogeneous half-space model

Figure 2 shows the sensitivity pattern of a homogeneous half-space model of 50 Ωm represented in Figure 1(a) for different configurations. From the numerical results, it is noticed that for all the configurations, the highest sensitivity values are found near both the potential and current electrodes. At larger distances from the electrodes, the contour patterns are different for the different arrays. In addition, the effective depth of measurement is sequentially increased by increasing the distance between the receiving electrodes and the transmitting electrodes. The farther is distance, the greater the vertical interval in which the bulk of the current flows. One important observation can be made when considering the sensitivity sections, that is, the negative sensitivity between the source electrode and receiving electrode and positive sensitivity between the source and potential electrode pairs.

Figure 2(a) indicates the sensitivity plot corresponding to the pole-pole array. Comparing the sensitivity patterns, it is observed that this array has the widest horizontal coverage and the deepest depth of investigation. However, it has the poorest resolution, which is reflected by the comparatively large spacing between the contours in the sensitivity function plot. The asymmetrical nature of the pole-dipole array is evident in the sensitivity section which is due to a remote current electrode (see Figure 2(b)). From the sensitivity function, it is obvious that analogous to dipole-dipole this array has almost vertical contours, but a larger depth of investigation compared to the dipole-dipole array. For the pole-dipole array with large receiver-transmitter separation, the region with the highest positive sensitivity values concentrate below the potential electrode pair. Referring to Figure 2(c), the dipole-dipole array has almost vertical contours beneath the center of the array meaning that the dipole-dipole configuration is more sensitive to vertical structures than to horizontal structures. Contrary to the dipole-dipole array, the sensitivity pattern of Wenner is almost horizontal leading to better detection of horizontal anomalies, but poor recognition of vertical anomalies (see Figure 2(d)).

b) Rectangular body model

The second inhomogeneous example includes one embedded block with the resistivity of 10 Ωm buried in 100 Ωm half-space at 1.2 m from the ground surface (Figure 1(b)). The object of this example is to investigate the sensitivity function of different arrays with respect to vertical structures. From Figure 3, it is concluded that the presence of inhomogeneity causes the distortion of the sensitivity pattern compared to a homogeneous medium. In addition, our numerical experiments demonstrate that the dipole-dipole and pole-dipole configurations have almost vertical contours indicating its higher sensitivity to vertical structures than to horizontal structures.

CONCLUSIONS

We proposed and formulated a numerical method using the element stiffness matrices and the potential distribution obtained from the finite difference modeling to calculate the sensitivity matrix values. The sensitivity distribution was computed for 2.5D electrical resistivity modeling in terms of different surface electrical configurations. To verify the proposed numerical algorithm, the sensitivity patterns of homogeneous and inhomogeneous models were provided. From our numerical experiments, it was shown that 1) the pole-pole array has the maximum penetration depth but the lowest horizontal and vertical resolution, 2) contrary to the pole-dipole and dipole-dipole arrays, Wenner is more sensitive to vertical changes than to horizontal changes, that is, the horizontal structures would be better detected by Wenner, 3) deformation of the sensitivity distributions is inevitable in the presence of inhomogeneity.

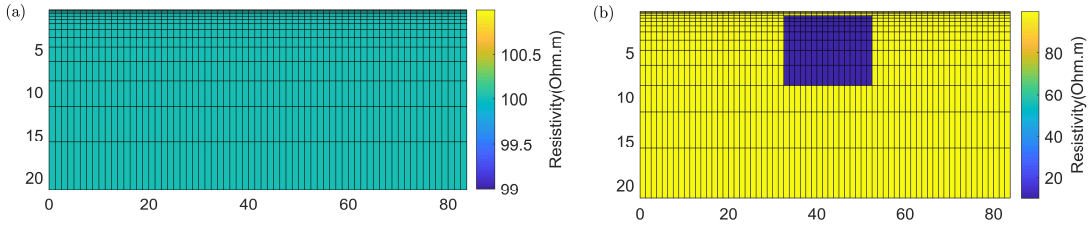

Figure 1. Representation of the simulated structures a) homogeneous half-space model, b) three-layered model, and c) rectangular body model.

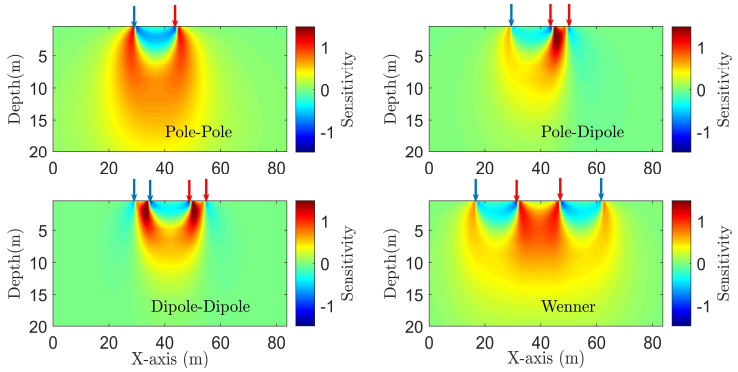

Figure 2. Normalized sensitivity patterns associated with a homogeneous half-space of 100 Ωm for a) pole-pole, b) pole-dipole, c) dipole-dipole, and d) wenner arrangement with electrode spacing of 5 m and $n = 3$ (where n is the number of receiver-transmitter separation). The blue and red arrows represent current and potential electrode location.

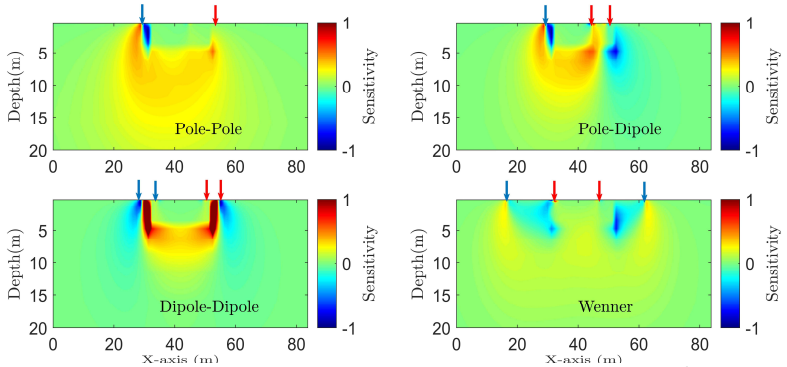

Figure 3. Normalized sensitivity patterns associated with a rectangular body model ($\frac{\rho_{body}}{\rho_{background}} = 0.1$) for a) pole-pole, b) pole-dipole, c) dipole-dipole, and d) wenner arrangement with electrode spacing of 5 m and $n = 3$ (where n is the number of receiver-transmitter separation). The blue and red arrows represent current and potential electrode location.

REFERENCES

Ghanati, R., Azadi, Y., Fakhimi, R., 2020. RESIP2DMODE: A MATLAB-Based 2D Resistivity and Induced Polarization Forward Modeling Software, Iranian Journal of Geophysics 13 (4), 60-78.

Günther, T., Rücker, C., and Spitzer, K., 2006. Three-dimensional modelling and inversion of dc resistivity data incorporating topography – II. Inversion. Geophys. J. Int., 166, 506–517.

Loke, M.H., Barker, R.D., 1995. Least-squares deconvolution of apparent resistivity pseudosections: Geophysics, 60, 1682–1690.

McGillivray, P.R., Oldenburg, D.W., 1990. Methods for calculating Fréchet derivatives and sensitivities for the non-linear inverse problem: a comparative study. Geophys. Prospect., 38(5):499–524.

Spitzer, K. (1998). The three-dimensional DC sensitivity for surface and subsurface sources. Geophys. J. Int., 134(3):736–746.

Szalai, S., Szarka, L., 2008. Parameter sensitivity maps of surface geo-electric arrays I. Linear arrays. Acta Geodaetica et Geophysica, 43, 419–437.